

# Sign Switchable Magnon Thermal Hall Conductivity in An Antiferromagnet

N. Li<sup>1,8</sup>, S. K. Guang<sup>1,8</sup>, W. J. Chu<sup>1</sup>, Q. Huang<sup>3</sup>, J. Liu<sup>3</sup>, K. Xia<sup>1</sup>, X. H. Zhou<sup>1</sup>, X. Y. Yue<sup>2</sup>, Y. Sun<sup>2</sup>, Y. Y. Wang<sup>2</sup>, Q. J. Li<sup>4</sup>, G. T. Lin<sup>5</sup>, J. Ma<sup>5</sup>, X. Zhao<sup>6\*</sup>, H. D. Zhou<sup>3\*</sup>, and  
X. F. Sun<sup>1,2,7\*</sup>

<sup>1</sup>Department of Physics, Hefei National Laboratory for Physical Sciences at Microscale, and Key Laboratory of Strongly-Coupled Quantum Matter Physics (CAS), University of Science and Technology of China, Hefei, Anhui 230026, People's Republic of China

<sup>2</sup>Institute of Physical Science and Information Technology, Anhui University, Hefei, Anhui 230601, People's Republic of China

<sup>3</sup>Department of Physics and Astronomy, University of Tennessee, Knoxville, Tennessee 37996-1200, USA

<sup>4</sup>School of Physics and Material Sciences, Anhui University, Hefei, Anhui 230601, People's Republic of China

<sup>5</sup>Key Laboratory of Artificial Structures and Quantum Control, Shenyang National Laboratory for Materials Science, School of Physics and Astronomy, Shanghai Jiao Tong University, Shanghai 200240, People's Republic of China

<sup>6</sup>School of Physical Sciences, University of Science and Technology of China, Hefei, Anhui 230026, People's Republic of China

<sup>7</sup>Collaborative Innovation Center of Advanced Microstructures, Nanjing University, Nanjing, Jiangsu 210093, People's Republic of China

<sup>8</sup>These authors contributed equally: N. Li, S. K. Guang.

\*email: xiazhao@ustc.edu.cn; hzhou10@utk.edu; xfsun@ustc.edu.cn

**While charge carriers in metals and semiconductors have been used as building blocks of modern technologies, the efforts to study and apply other particles or quasiparticles, such as the magnons (the quanta of spin waves) in magnets, for next generation of technologies have been going on for decades. One fundamental**

**question for the magnon is whether it exhibits the Hall effect, which is usually driven by the Lorentz force; therefore, as a charge-free quasiparticle, magnon may be expected not to lead to it. Recently several ferromagnetic ordered materials have been reported to exhibit magnon Hall effect, such as the thermal Hall conductivity  $\kappa_{xy}$ . However, whether the magnon Hall effect exists in antiferromagnetic ordered materials, another big branch of magnets, is still illusive. Here, we reported a  $\kappa_{xy}$  in the antiferromagnetic ordered state of  $\text{Na}_2\text{Co}_2\text{TeO}_6$ . This  $\kappa_{xy}$  shows peculiar behaviors including sign changes induced both by temperature and field, non-monotonic field dependence, and a thermal Hall angle reaching 2%, all of which strongly support its magnon origin. Therefore,  $\text{Na}_2\text{Co}_2\text{TeO}_6$  not only provides a unique opportunity for studying magnon Hall effect in antiferromagnets but also a platform for potential magnonics applications.**

In recent years, magnonics, studies on the excitation, propagation, control and detection of spin waves (quanta of which are called magnons), have received intensive attentions<sup>1-4</sup>. This subject is important not only for basic research for better understanding the quantum magnetic dynamic phenomena but also for future technologies since magnons are promising information carriers with the advantages of low energy consumption and long coherence length<sup>5,6</sup>. One fundamental question for the magnon, a charge-free quasi-particle, is whether it exhibits Hall effect, which is usually driven by the Lorentz force. While theoretical studies have predicted magnon Hall effect, such as the thermal Hall conductivity,  $\kappa_{xy}$ , in various magnets<sup>7-17</sup>, experimentally the  $\kappa_{xy}$  has only been observed in several systems including pyrochlore  $\text{Lu}_2\text{V}_2\text{O}_7$ <sup>18</sup>, kagome  $\text{Cu}(1-3, \text{bdc})$ <sup>19</sup>, and honeycomb  $\text{VI}_3$ <sup>20</sup>. In fact, all these three systems are ferromagnetic (FM) ordered materials, in which the  $\kappa_{xy}$  is generated by the Berry curvature of magnons arising from the Dzyaloshinskii-Moriya interaction (DMI) on different lattices. On the other hand, whether magnon Hall effect exists in the antiferromagnetic (AFM) ordered state of antiferromagnets, which certainly is a big branch of magnetic materials, is not clear and short of studies.

The  $\kappa_{xy}$  has been reported for one AFM ordered material, the honeycomb compound  $\alpha$ -RuCl<sub>3</sub>. It has been intensively studied recently as it has been suggested to host a proximate Kitaev quantum spin liquid (QSL)<sup>21-23</sup>, a new state of matter where long range magnetic ordering is suppressed due to substantial quantum fluctuations approaching zero temperature<sup>24-26</sup>. The reported  $\kappa_{xy}$  occurs in its paramagnetic state and switches sign around its AFM ordering temperature  $T_N = 7$  K<sup>27,28</sup>. Moreover, it reaches a half-integer quantization of the thermal Hall conductance in the field induced disordered state<sup>29,30</sup>. The origin of this  $\kappa_{xy}$  observed in these spin disordered states has been linked to the itinerant Majorana fermions on a honeycomb lattice predicted by the Kitaev model<sup>13</sup>. However, the most recently reported  $\kappa_{xy}$  shows no such sign change around  $T_N$ <sup>31,32</sup>. Czajka *et al.*<sup>31</sup> proposed that the  $\kappa_{xy}$  is due to bosonic edge excitations, which is incompatible with the half-integer quantization. Lefrancois *et al.*<sup>32</sup> proposed a phonon origin of the  $\kappa_{xy}$  since it mirrors the temperature evolution of the phonon dominated  $\kappa_{xx}$  very well. These contradictory results cast doubt on the existence of magnon thermal Hall effect in the AFM ordered state of  $\alpha$ -RuCl<sub>3</sub>.

Here, we reported a  $\kappa_{xy}$  in the AFM ordered state below  $T_N$  of Na<sub>2</sub>Co<sub>2</sub>TeO<sub>6</sub> (NCTO), which is an effective spin-1/2 (Co<sup>2+</sup>) honeycomb magnet (Figure 1a). The peculiar behaviors of  $\kappa_{xy}$ , including sign changes induced not only by temperature but also by field, non-monotonic field dependence, and a thermal Hall angle reaching as large as 2%, strongly support its magnon origin. We propose this  $\kappa_{xy}$  is generated by the Berry curvature of the magnons due to NCTO's dominant Kitaev coupling. Our observation represents a rare case about magnon thermal Hall effect in an AFM ordered state.

Figure 1c shows the temperature dependence of longitudinal thermal conductivity  $\kappa_{xx}(T)$  of NCTO at zero field. The previous studies show that NCTO enters an AFM ordered state with zigzag spin structure below  $T_N = 27$  K, followed by two possible spin re-orientation around 16 K and 4 K, respectively<sup>33-36</sup>. Our  $\kappa_{xx}(T)$  data shows no obvious anomaly around 27 K and 16 K, similar to the reported  $\kappa_{xx}(T)$  data<sup>37</sup>, but a clear kink around 3 K that could be related to the spin re-orientation at 4 K<sup>33,35</sup>. At subkevin temperatures, the  $\kappa_{xx}$  shows a roughly  $T^{1.2}$  behavior, which is different from the  $T^3$

behavior that is expected for both the phonon and magnon thermal conductivity at low temperatures. Therefore, this  $T^{1.2}$  behavior indicates the existence of magnon scattering of phonons.

Figures 1d and 1e show the field dependence of  $\kappa_{xx}$  measured at various temperatures with  $B // c$ . At  $T < 1.56$  K, the  $\kappa_{xx}(B)$  decreases quickly with increasing fields to reach a minimum around 4 T, and then shows a weak field dependence up to 14 T. At 2.2 K, 2.7 K and 3.2 K, the  $\kappa_{xx}(B)$  shows a double-valley structure with valleys around 2 T and 10 T, respectively. At even higher temperatures, the  $\kappa_{xx}(B)$  exhibits a broad valley around 5 ~ 10 T. The reported magnetization measured at 2 K with  $B // c$  of NCTO shows no obvious anomaly up to 30 T but indicates to enter a FM state around 13 T that should be related to the closure and re-opening of a spin gap<sup>38</sup>. Indeed, the inelastic neutron scattering experiments have revealed a spin gap of 0.4 meV in NCTO<sup>39,40</sup>. With increasing field, the gradual closing of the spin gap leads to the increase of low-energy magnon excitations which could have two effects, one is to enhance  $\kappa_{xx}$  if magnon itself conducts heat and the other is to suppress  $\kappa_{xx}$  if magnon scatters phonon. Since the magnetization data shows no sign of spin structure change at low fields, we propose the valley at low fields is a resonant peak due to the competition of these two effects. The high field valley around 10 T then should be related to the gap closure and re-opening where  $\kappa_{xx}$  usually reaches a minimum.

Figures 2a and 2b show the field dependence of the thermal Hall conductivity  $\kappa_{xy}$  at various temperatures below  $T_N$ . At  $T \leq 2.2$  K, with increasing field, the  $\kappa_{xy}(B)$  first exhibits a negative Hall response to reach a negative maximum around 3 ~ 5 T; then it switches sign to be positive around 10 T and increases at higher fields. At 3.2 K and 5.4 K, the  $\kappa_{xy}$  curves show a positive peak at low fields, followed by two zero crossings with increasing fields. At 7.8 K, the  $\kappa_{xy}$  is positive without sign change. The temperature dependence of  $\kappa_{xy}/T$  at several fields is shown in Figure 2c. It is clear that at  $B = 3$  and 5 T, with increasing temperature,  $\kappa_{xy}$  is negative and reaches a dip around 2 ~ 3 K, and then switches sign to be positive around 3 ~ 4 K. Figure 2d shows the field dependence of the thermal Hall angle,  $\kappa_{xy} / \kappa_{xx}$ , at various temperatures. At  $T \leq 2.2$  K, all curves

consistently show a maximum negative value at 4 T and switch sign to be positive around 10 T. The highest absolute value of  $\kappa_{xy}/\kappa_{xx}$  is around 2% at 0.78 K and 4 T.

As a good insulator, there are several possible origins for the  $\kappa_{xy}$  observed in NCTO, including phonons, magnons, and fractionalized exotic quasiparticles such as spinons. In general, the  $\kappa_{xy}$  caused by phonons or magnon scattering of phonons is expected to increase monotonically with increasing field and shows no sign change<sup>41-45</sup>. For spinon  $\kappa_{xy}$ , it only has been observed in spin liquid state with disordered spins<sup>46-49</sup>. Apparently, these two scenarios cannot explain the sign-switchable and non-monotonic  $\kappa_{xy}$  observed in the AFM ordered state of NCTO. Therefore, the  $\kappa_{xy}$  in NCTO must originate from its magnons.

The former theoretical studies on honeycomb magnets by using the Kitaev-Heisenberg model (the  $J_1$ - $K$ - $\Gamma$ - $J_3$  model, here  $J_1$  ( $J_3$ ) is the nearest-neighbor (third-nearest-neighbor) Heisenberg coupling;  $K$  and  $\Gamma$  are the nearest-neighbor Kitaev and symmetric off-diagonal couplings, respectively.) have proposed that with dominant Kitaev coupling, the  $\kappa_{xy}$  could be generated by the Berry curvature of the magnons<sup>50,51</sup>. In fact, Li and Okamoto<sup>51</sup> show that with certain spin structure and zero or weak spin-phonon interactions, the calculated  $\kappa_{xy}$  based on this model is negative at low temperatures, which reaches a dip and switches sign to be positive with increasing temperature. This is similar to the  $\kappa_{xy}$  behavior presented above for NCTO. While this calculation was checked by using couplings of  $\alpha$ -RuCl<sub>3</sub> with  $J_1 = -0.5$  meV,  $K = -5.0$  meV,  $J_3 = 0.5$  meV, and  $\Gamma = 2.5$  meV, it should provide guidance to the  $\kappa_{xy}$  behavior of NCTO too since the recent studies show that NCTO also has dominant Kitaev coupling with  $J_1 = -0.2$  meV,  $K = -7.0$  meV,  $J_3 = 1.6$  meV, and  $\Gamma = 0.5$  meV<sup>52</sup>. Therefore, we propose that the Berry curvature of the magnons led by the dominant Kitaev coupling on its honeycomb lattice is the origin for the observed  $\kappa_{xy}$  in NCTO. Its sign changes should be related to the Berry curvature changes caused by either the thermal effects (for the one induced by temperature around 3 ~ 4 K) or the entrance to the FM state from the AFM ordered state (for the one induced by field around 10 T).

At last, the 2% thermal Hall angle is exceptional large for an insulator. The typical

value of the thermal Hall angle for an insulator, either originates from phonon or magnon, is typically around 0.3% ~ 0.6% or lower<sup>53</sup>. Only in the pyrochlore  $\text{Yb}_2\text{Ti}_2\text{O}_7$ , a 2% thermal Hall angle was reported in its spin liquid state<sup>49</sup>.

In summary, NCTO is a rare AFM insulator exhibiting magnon thermal Hall effect in its AFM ordered state. Its sign can be switched both by temperature and field and its thermal Hall angle reaches a maximum value around 2%. These features, plus its quasi-two dimensional structure, demonstrate that NCTO could be a promising platform for future magnonics applications.

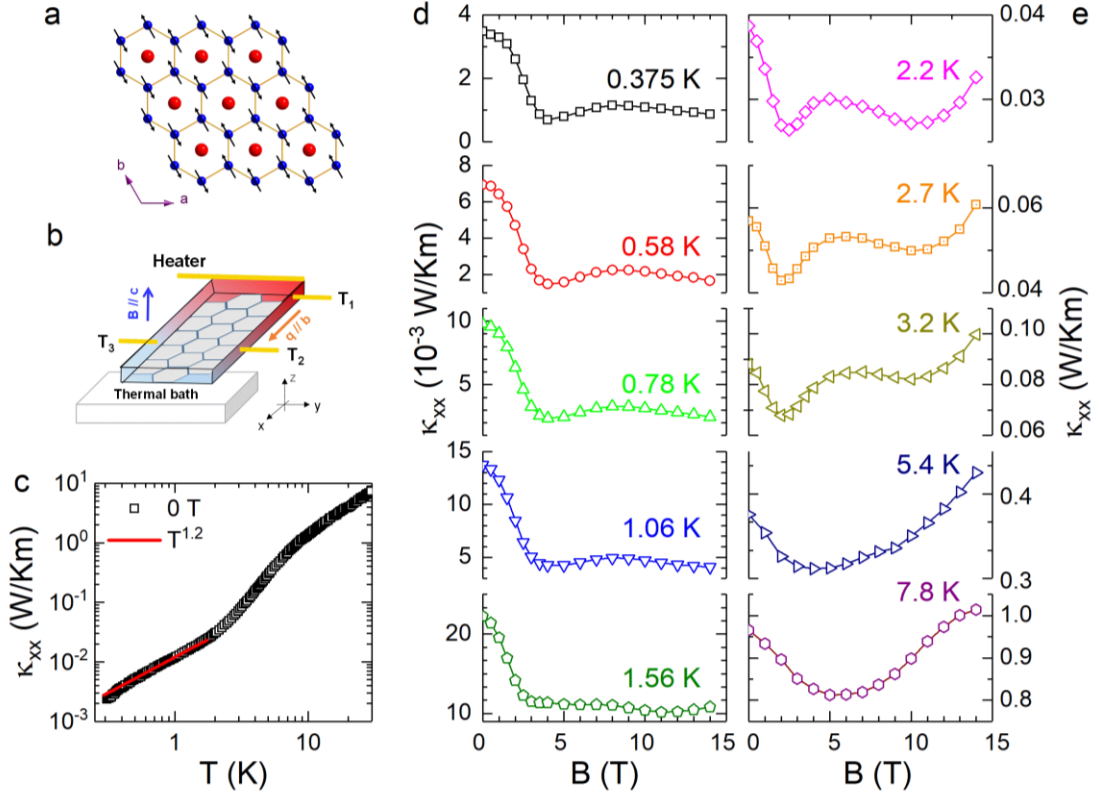


**Figure 1** Longitudinal thermal conductivity  $\kappa_{xx}$  of  $\text{Na}_2\text{Co}_2\text{TeO}_6$  single crystals. **a**, Crystallographic spin structure of the  $ab$  plane of  $\text{Na}_2\text{Co}_2\text{TeO}_6$  in the AFM state. The honeycomb lattice consists of Co ions (blue spheres) with the zigzag AFM arrangements (the arrows indicated) and the Te ions (red spheres) locate at the center of each honeycomb lattice. **b**, Schematic of the experimental setup for thermal Hall measurement. The heat current was applied along the  $b$  axis and the magnetic field was applied along the  $c$  axis. The longitudinal and transverse temperature gradients are determined by the difference between  $T_1$  and  $T_2$  and between  $T_2$  and  $T_3$ , respectively. **c**, Temperature dependence of the longitudinal thermal conductivity  $\kappa_{xx}$  in zero field. The zero-field data display a rough  $T^{1.2}$  behavior at very low temperatures, indicated by the solid line. **d,e**, Magnetic-field dependence of thermal conductivity at various temperatures and with  $B // c$ .

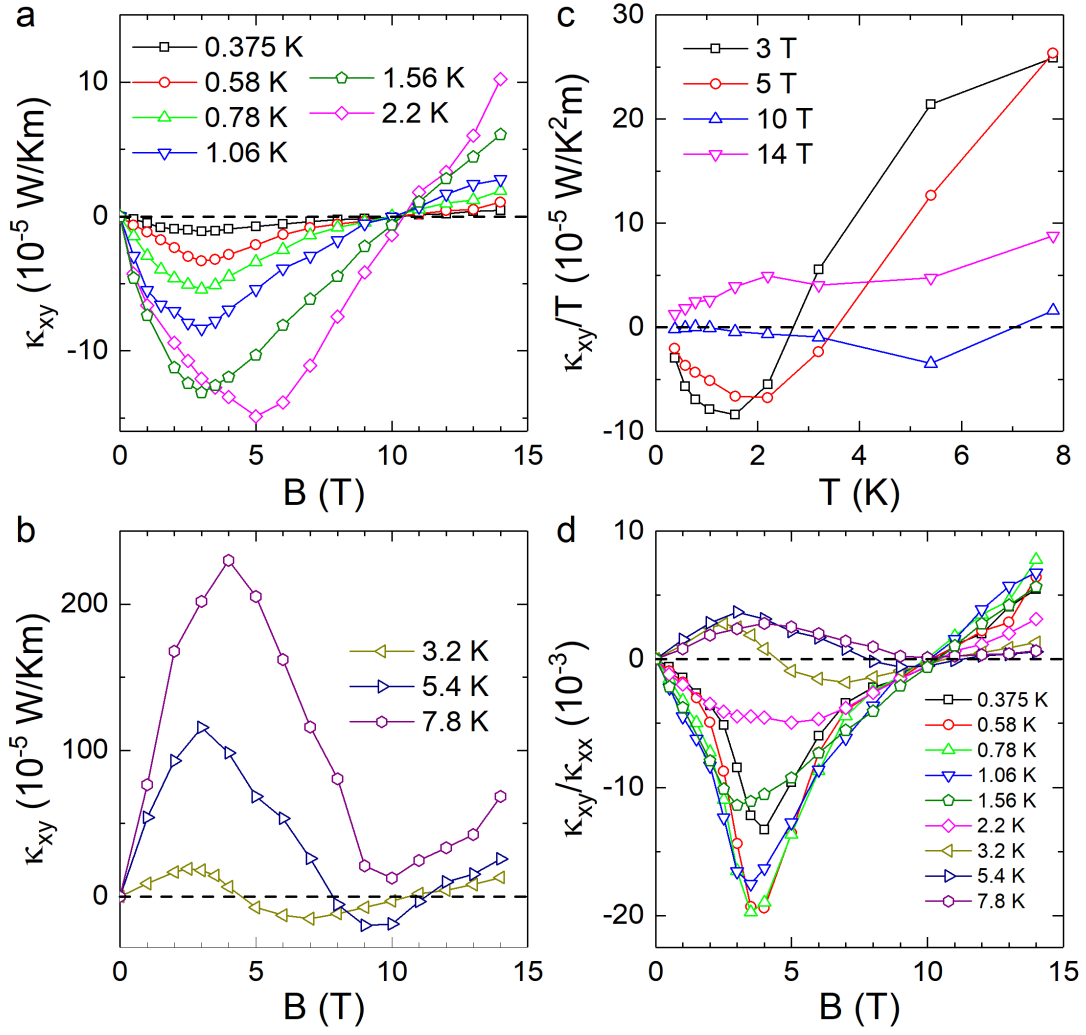


**Figure 2 Thermal Hall conductivity of  $\text{Na}_2\text{Co}_2\text{TeO}_6$  single crystal.** **a,b,** Field dependence of thermal Hall conductivity  $\kappa_{xy}$  for  $B // c$  at various temperatures. There are sign reversals of  $\kappa_{xy}$  upon changing magnetic field. **c,** Temperature dependence of  $\kappa_{xy}/T$  at select magnetic fields. There are also sign reversals with changing temperature. **d,** Temperature dependence of the thermal Hall angle  $\kappa_{xy}/\kappa_{xx}$ . All dashed lines are guide to the eyes.

## Methods

**Single crystal growth.** The polycrystalline sample of NCTO was mixed with the flux of Na<sub>2</sub>O and TeO<sub>2</sub> in a molar ratio of 1:0.5:2 and gradually heated to 900 °C at 3 °C/minute in the air after grinding. The sample was retained at 900 °C for 30 hours and was cooled to a temperature of 500 °C at the rate of 3 °C/hour. The furnace was then shut down to cool to room temperature. The obtained NCTO single crystals are thin plates with hexagonal geometry.

**Heat transport measurements.** A thin-plate shaped crystal with size of  $6.3 \times 2.17 \times 0.053$  mm<sup>3</sup> was used for heat transport measurements. The longitudinal thermal conductivity and thermal Hall conductivity were measured simultaneously by using the standard steady-state technique with “one heater, three thermometers”. Heat current and magnetic field were applied along the *b* and *c* axes, respectively (see the illustration in Figure 1b). The crystallinity directions were determined by the X-ray Laue photograph. The longitudinal and transverse temperature gradients were measured by three in-situ calibrated RuO<sub>2</sub> thermometers. The measurements were carried out in a <sup>3</sup>He refrigerator equipped with a 14 T magnet. The longitudinal thermal conductivity  $\kappa_{xx}$  and thermal hall conductivity  $\kappa_{xy}$  were obtained by the following formals<sup>47</sup>

$$\omega_{xx} = \nabla_x T / q,$$

$$\omega_{xy} = \nabla_y T^{\text{asym}} / q,$$

$$\kappa_{xx} = \omega_{xx} / (\omega_{xx}^2 + \omega_{xy}^2),$$

$$\kappa_{xy} = -\omega_{xy} / (\omega_{xx}^2 + \omega_{xy}^2),$$

where  $q$ ,  $\nabla_x T$ ,  $\omega_{xx}$  and  $\omega_{xy}$  are the heat current, longitudinal temperature gradients, longitudinal thermal resistivity and thermal Hall resistivity, respectively. In order to avoid the longitudinal response originated from the misalignment of two transverse contacts, the relationship  $\nabla_y T^{\text{asym}}(B) = [\nabla_y T(B) - \nabla_y T(-B)]$  was used to subtract the field-symmetric component. All  $\kappa_{xx}$  and  $\kappa_{xy}$  curves were measured with zero-field cooling to the fixed temperatures from 30 K.

## Data availability

The data that support the findings of this study are available from the corresponding author upon reasonable request.

## References

1. Demokritov, S. O. & Slavin, A. N. Magnonics: From Fundamentals to Applications, Topics in Applied Physics Vol. **125** (Springer, New York, 2013).
2. Kruglyak, V. V., Demokritov, S. O. & Grundler, D. Magnonics. *J. Phys. D* **43**, 264001 (2010).
3. Wang, X. S., Zhang, H. W. & Wang, X. R. Topological magnonics: a paradigm for spin-wave manipulation and device design. *Phys. Rev. Applied* **9**, 024029 (2018).
4. Barman, A. *et al.* The 2021 magnonics roadmap. *J. Phys. Condens. Matt.* **33**, 413001 (2021).
5. Kajiwara, Y. *et al.* Transmission of electrical signals by spin-wave interconversion in a magnetic insulator. *Nature* **464**, 262-266 (2010).
6. Yan, P., Wang, X. S. & Wang, X. R. All-magnonic spin-transfer torque and domain wall propagation. *Phys. Rev. Lett.* **107**, 177207 (2011).
7. Fujimoto, S. Hall effect of spin waves in frustrated magnets. *Phys. Rev. Lett.* **103**, 047203 (2009).
8. Katsura, H., Nagaosa, N. & Lee, P. A. Theory of the thermal Hall effect in quantum magnets. *Phys. Rev. Lett.* **104**, 066403 (2010).
9. Matsumoto, R. & Murakami, S. Theoretical prediction of a rotating magnon wave packet in ferromagnets. *Phys. Rev. Lett.* **106**, 197202 (2011).
10. Mook, A., Henk, J. & Mertig, I. Magnon Hall effect and topology in kagome lattices: A theoretical investigation. *Phys. Rev. B* **89**, 134409 (2014).
11. Owerre, S. A. Topological honeycomb magnon Hall effect: A calculation of thermal Hall conductivity of magnetic spin excitations. *J. Appl. Phys.* **120**, 043903 (2016).
12. Zyuzin, V. A. & Kovalev, A. A. Magnon spin Nernst effect in antiferromagnets. *Phys.*

- Rev. Lett.* **117**, 217203 (2016).
13. Nasu, J., Yoshitake, J. & Mtome, Y. Thermal transport in the Kitaev model. *Phys. Rev. Lett.* **119**, 127204 (2017).
  14. Laurell, P. & Fiete, G. A. Magnon thermal Hall effect in kagome antiferromagnets with Dzyaloshinskii-Moriya interactions. *Phys. Rev. B* **98**, 094419 (2018).
  15. Hwang, K., Trivedi, N. & Randeria, M. Topological magnons with nodal-line and triple-point degeneracies: implications for thermal Hall effect in pyrochlore iridates. *Phys. Rev. Lett.* **125**, 047203 (2020).
  16. Carnahan, C., Zhang, Y. & Xiao, D. Thermal Hall effect of chiral spin fluctuations. *Phys. Rev. B* **103**, 224419 (2021).
  17. Nakata, K. & Kim, S. K. Topological Hall effects of magnons in ferrimagnets. *J. Phys. Soc. Jpn.* **90**, 081004 (2021).
  18. Onose, Y. *et al.* Observation of the magnon Hall effect. *Science* **329**, 297-299 (2010).
  19. Hirschberger, M., Chisnell, R., Lee, Y. S. & Ong, N. P. Thermal Hall Effect of Spin Excitations in a Kagome Magnet. *Phys. Rev. Lett.* **115**, 106603 (2015).
  20. Zhang, H. *et al.* Anomalous Thermal Hall Effect in an Insulating van der Waals Magnet. *Phys. Rev. Lett.* **127**, 247202 (2021).
  21. Kitaev, A. Anyons in an exactly solved model and beyond. *Ann. Phys.* **321**, 2-111 (2006).
  22. Balents, L. Spin liquids in frustrated magnets. *Nature* **464**, 199-208 (2010).
  23. Savary, L. & Balents, L. Quantum spin liquids: a review. *Rep. Prog. Phys.* **80**, 016502 (2016).
  24. Zhou, Y., Kanoda, K. & Ng, T.-K. Quantum spin liquid states. *Rev. Mod. Phys.* **89**, 025003 (2017).
  25. Banerjee, A. *et al.* Proximate Kitaev quantum spin liquid behaviour in a honeycomb magnet. *Nat. Mater.* **15**, 733-740 (2016).
  26. Banerjee, A. *et al.* Neutron scattering in the proximate quantum spin liquid  $\alpha$ - $\text{RuCl}_3$ . *Science* **356**, 1055-1059 (2017).

27. Kasahara, Y. *et al.* Unusual thermal Hall effect in a Kitaev spin liquid candidate  $\alpha$ -RuCl<sub>3</sub>. *Phys. Rev. Lett.* **120**, 217205 (2018).
28. Hentrich, R. *et al.* Large thermal Hall effect in  $\alpha$ -RuCl<sub>3</sub>: evidence for heat transport by Kitaev-Heisenberg paramagnons. *Phys. Rev. B* **99**, 085136 (2019).
29. Kasahara, Y. *et al.* Majorana quantization and half-integer thermal quantum Hall effect in a Kitaev spin liquid. *Nature* **559**, 227-231 (2018).
30. Yokoi, T. *et al.* Half-integer quantized anomalous thermal Hall effect in the Kitaev material candidate  $\alpha$ -RuCl<sub>3</sub>. *Science* **373**, 568-572 (2021).
31. Czajka, P. *et al.* The planar thermal Hall conductivity in the Kitaev magnet  $\alpha$ -RuCl<sub>3</sub>. arXiv:2201.07873 (2022).
32. Lefrançois, É. *et al.* Evidence of a Phonon Hall Effect in the Kitaev Spin Liquid Candidate  $\alpha$ -RuCl<sub>3</sub>. arXiv:2111.05493 (2021).
33. Lefrançois, É. *et al.* Magnetic properties of the honeycomb oxide Na<sub>2</sub>Co<sub>2</sub>TeO<sub>6</sub>. *Phys. Rev. B* **94**, 214416 (2016).
34. Viciu, L. *et al.* Structure and basic magnetic properties of the honeycomb lattice compounds Na<sub>2</sub>Co<sub>2</sub>TeO<sub>6</sub> and Na<sub>3</sub>Co<sub>2</sub>SbO<sub>6</sub>. *J. Solid State Chem.* **180**, 1060-1067 (2007).
35. Xiao, G. *et al.* Crystal growth and the magnetic properties of Na<sub>2</sub>Co<sub>2</sub>TeO<sub>6</sub> with quasi-two-dimensional honeycomb lattice. *Cryst. Growth Des.* **19**, 2658-2662 (2019).
36. Yao, W. & Li, Y. Ferrimagnetism and anisotropic phase tunability by magnetic fields in Na<sub>2</sub>Co<sub>2</sub>TeO<sub>6</sub>. *Phys. Rev. B* **101**, 085120 (2020).
37. Hong, X. *et al.* Strongly scattered phonon heat transport of the candidate Kitaev material Na<sub>2</sub>Co<sub>2</sub>TeO<sub>6</sub>. *Phys. Rev. B* **104**, 144426 (2021).
38. Xiao, G. *et al.* Magnetic properties and phase diagram of quasi-two-dimensional Na<sub>2</sub>Co<sub>2</sub>TeO<sub>6</sub> single crystal under high magnetic field. *J. Phys.: Condens. Matt.* **34**, 075801 (2022).

39. Kim, C. *et al.* Antiferromagnetic Kitaev interaction in  $J_{\text{eff}} = 1/2$  cobalt honeycomb materials  $\text{Na}_3\text{Co}_2\text{SbO}_6$  and  $\text{Na}_2\text{Co}_2\text{TeO}_6$ . *J. Phys.: Condens. Matt.* **34**, 045802 (2022).
40. Lin, G. *et al.* Field-induced quantum spin disordered state in spin-1/2 honeycomb magnet  $\text{Na}_2\text{Co}_2\text{TeO}_6$ . *Nat. Commun.* **12**, 5559 (2021).
41. Li, X., Fauqué, B., Zhu, Z. & Behnia, K. Phonon thermal Hall effect in strontium titanate. *Phys. Rev. Lett.* **124**, 105901 (2020).
42. Strohm, C., Rikken, G. L. J. & Wyder, P. Phenomenological evidence for the phonon Hall effect. *Phys. Rev. Lett.* **95**, 155901 (2005).
43. Mori, M., Spencer-Smith, A., Sushkov, O. P. & Maekawa, S. Origin of the phonon Hall effect in rare-earth garnets. *Phys. Rev. Lett.* **113**, 265901 (2014).
44. Sugii, K. *et al.* Thermal Hall effect in a phonon-glass  $\text{Ba}_3\text{CuSb}_2\text{O}_9$ . *Phys. Rev. Lett.* **118**, 145902 (2017).
45. Ideue, T., Kurumaji, T., Ishiwata, S. & Tokura, Y. Giant thermal Hall effect in multiferroics. *Nat. Mater.* **16**, 797-803 (2017).
46. Watanabe, D. *et al.* Emergence of nontrivial magnetic excitations in a spin-liquid state of kagomé volborthite. *Proc. Natl. Acad. Sci. U. S. A.* **113**, 8653-8657 (2016).
47. Doki, H. *et al.* Spin thermal Hall conductivity of a kagome antiferromagnet. *Phys. Rev. Lett.* **121**, 097203 (2018).
48. Hirschberger, M., Krizan, J. W., Cava, R. J. & Ong, N. P. Large thermal Hall conductivity of neutral spin excitations in a frustrated quantum magnet. *Science* **348**, 106-109 (2015).
49. Hirschberger, M., Czajka, P., Koohpayeh, S. M., Wang, W. & Ong, N. P. Enhanced thermal Hall conductivity below 1 Kelvin in the pyrochlore magnet  $\text{Yb}_2\text{Ti}_2\text{O}_7$ . arXiv:1903.00595 (2019).
50. Cookmeyer, J. & Moore, J. E. Spin-wave analysis of the low-temperature thermal Hall effect in the candidate Kitaev spin liquid  $\alpha\text{-RuCl}_3$ . *Phys. Rev. B* **98**, 060412(R) (2018).

51. Li, S. & Okamoto, S. Thermal Hall effect in the Kitaev-Heisenberg system with spin-phonon coupling. arXiv:2112.06107 (2021).
52. Sanders, A. L. *et al.* Dominant Kitaev interactions in the honeycomb materials  $\text{Na}_3\text{Co}_2\text{SbO}_6$  and  $\text{Na}_2\text{Co}_2\text{TeO}_6$ . arXiv:2112.12254 (2021).
53. Chen, L., Boulanger, M. E., Wang, Z. C., Tafti, F. & Taillefer, L. Large phonon thermal Hall conductivity in a simple antiferromagnetic insulator. arXiv:2110.13277 (2021).

### **Acknowledgements**

This work was supported by the National Natural Science Foundation of China (Grant Nos. U1832209, 11874336, 12174361, 12104010, 12104011, 12025408, and 11904003) and the Nature Science Foundation of Anhui Province (Grant Nos. 1908085MA09 and 2108085QA22). The work at the University of Tennessee was supported by U.S. Department of Energy under Award No. DE-SC-0020254.

### **Author contributions**

N.L., S.K.G., W.J.C., K.X., X.H.Z., X.Y.Y., Y.Y.W., Y.S., and Q.J.L. performed thermal conductivity measurements and analyzed the data with help from X.Z., X.F.S. and H.D.Z. Q.H., J.L., and H.D.Z. made the single-crystal samples. G.T.L. and J.M. performed the magnetic susceptibility and specific heat measurements. X.F.S., X.Z. and H.D.Z. wrote the paper with input from all other co-authors.

### **Competing financial interests**

The authors declare no competing financial interests.

### **Additional Information**

**Correspondence and requests for materials** should be addressed to H.D.Z., X.F.S. or X.Z.